Elsevier Editorial System(tm) for NeuroImage
Manuscript Draft

Manuscript Number:

Title: A model-free approach for identifying asymmetries in cross-dimensional functional consistency

Article Type: Full length article

Section/Category: Analysis Methods

Corresponding Author: Mr. Matan Mazor, MSc

Corresponding Author's Institution: Tel Aviv University

First Author: Matan Mazor, MSc

Order of Authors: Matan Mazor, MSc; Roy Mukamel, PhD

Abstract: Functional magnetic resonance imaging (fMRI) experiments are typically designed to allow the extraction of evoked responses to isolated experimental conditions. At the experimental design level, this is achieved in two ways: randomizing the order of experimental conditions within and between runs, and using a sparse spread of events, allowing for the signal to decay between subsequent events or blocks (with the exception of fast-event related and neural adaptation designs). At the analysis level, a design matrix is constructed with one or more regressors for each experimental condition, and beta weights are then compared in a univariate (single voxel) or multivariate (multi-voxel) manner to assess sensitivity of a particular brain region to the different experimental manipulations. However, often a researcher is less interested in the differences in evoked responses to specific experimental conditions (e.g., observation of a red or blue square), but more in the sensitivity of a brain region to the manipulated experimental dimensions (e.g., color). To this end, we introduce a novel experimental design and analysis. Together, this new approach allows to infer from asymmetry in the inter-run temporal consistency pattern about sensitivity of single voxels to different experimental dimensions. This approach is model-free, making it appealing for the study of brain regions, populations and experimental manipulations in which assumptions about the hemodynamic response function do not hold. Here we applied it to study the lateralization of hand representation during action-observation. We discuss the possible strengths and limitations of this new approach, in light of our empirical results.

Suggested Reviewers: Nikolaus Kriegeskorte PhD
Programme leader, Memory and perception group, Congition and Brain Sciences Unit, University of Cambridge
nikolaus.kriegeskorte@mrc-cbu.cam.ac.uk
The proposed manuscript presents a novel temporal information-based approach to fMRI anlaysis. We find Prof. Kriegeskorte's work to be highly relevant to this project, in light of his contribution to information-based approaches to fMRI analysis, and his writing about theoretical aspects of multivariate analysis.

Karl J. Friston FMedSci FRSB FRS

Principal Investigator, Institute of Neurology, University College London
k.friston@ucl.ac.uk
The proposed manuscript presents a novel approach to fMRI analysis. We find Prof. Friston's extensive contribution to methodological and statistical aspects of inference from neuroimaging data to be highly relevant.

Uri Hasson PhD
Principal Investigator, Department of Psychology, Princeton University
hasson@princeton.edu
Here we use the correlations between time-series as an index of the sensitivity of a voxel to different experimental dimensions. Thus, previous works by Prof. Hasson on intra-subject and inter-subject correlations are highly relevant.

Jeanette Mumford PhD
Associate Scientist, Waisman Center, University of Wisconsin-Madison
jeanette.mumford@gmail.com
Dr. Mumford's input on this project will be especially valuable, given her expertise in statistical analysis of functional magnetic resonance imaging (fMRI) data.

Lior Shmuelof PhD
Head of Brain and Action Lab, Neuroscience, Ben Gurion University
shmuelof@bgu.ac.il
Dr. Shmuelof's previous work on the representation of hands from different perspectives is especially relevant to the experiment presented here, in which we applied TWISTER design and TCA to study how hand identity is represented in different regions of the human brain.

Opposed Reviewers:

Dear Editor, March 2017

We submit the enclosed manuscript titled "**A model free approach for identifying asymmetries in cross-dimensional functional consistency**" for potential publication as a manuscript in *Neuroimage*.

Common methods for fMRI analysis employ a *linear transform model* that assumes a specific linear relation between experimental events and the measured response in the brain. This simple model is successfully applied in mass univariate testing (standard GLM) and as a preliminary step to spatially multivariate methods (such as multi-voxel pattern analysis and representational similarity analysis). However, the model's assumptions (e.g., the principles of linearity and the shape of the hemodynamic response function) have been shown not to hold in certain subcortical structures, in special populations and age groups and following drug administration. In this paper we introduce a novel approach that obviates the need to model the signal by focusing on the experimental *dimensions*, instead on specific experimental *conditions*. The unique two-step scheme relies on a) using a special experimental design (TWISTER) that specifically manipulates the inter-run temporal consistency pattern along two experimental dimensions of interest, and b) analyzing the voxel-wise data using a specialized statistical method (Temporal Consistency Asymmetry; TCA) that targets asymmetries in the temporal consistency pattern in the time-series data as proxies for asymmetries in the voxel's representational space. This method has the following advantages:

1. TCA is a model-free analysis, and thus does not presuppose any specific relation between experimental events, cognitive processes, neural responses and the measured blood-oxygenation level dependent signal. This makes the combination of TWISTER design and TCA a promising direction for the study of different populations, age-groups, brain-regions (e.g., subcortical) and interventions (e.g., drug administration) that show consistent, but model-resistant activation patterns.
2. TCA extends the multivariate approach to neuroimaging (as employed in Multi-Voxel Pattern Analysis, or Representational Similarity Analysis) to the temporal domain, allowing for idiosyncratic temporal dynamics, including signal saturation and inter-trial interactions, to be discovered and successfully propagated to group-level inference.

3. TCA puts to test a strong, directional hypothesis, about specific asymmetries in the voxel's representational space. This is in contrast to multi-voxel pattern analysis, which tests the general hypothesis that a certain brain region does not hold any discriminating information regarding two conditions.

Here we used the combination of TWISTER design and TCA to study the lateralization of hand representation during action-observation. TCA successfully identified asymmetries in inter-run temporal consistency patterns at the single-subject and group-levels, for specific regions along the visual pathway. Furthermore, analyzing the same set of data using mass univariate GLM revealed results that partially overlap those discovered with the model-free TCA. Our results support the validity of this method as an additional tool for functional inference of neural structures, and its possible benefits for the study of subcortical structures.

We believe our results will be of high interest to a broad range of neuroscientists studying populations, interventions, or neural structures that show model-resistant temporal dynamics.

We suggest the following experts as potential reviewers:

1. Prof. Nikolaus Kriegeskorte
   (University of Cambridge; nikolaus.kriegeskorte@mrc-cbu.cam.ac.uk)
2. Prof. Karl J. Friston
   (University College London; k.friston@ucl.ac.uk)
3. Prof. Uri Hasson
   (Princeton University; hasson@princeton.edu)
4. Dr. Jeanette Mumford
   (University of Wisconsin-Madison; jeanette.mumford@gmail.com)
5. Prof. Lior Shmuelof
   (Ben-Gurion University; shmuelof@bgu.ac.il)

Thank you for considering this submission,
Sincerely,

Prof. Roy Mukamel,
School of Psychological Sciences and Sagol School of Neuroscience

Tel-Aviv University
Tel-Aviv 69978, Israel
Tel: +972-3-640-7246
rmukamel@tau.ac.il

A model-free approach for identifying asymmetries in cross-dimensional functional consistency

Matan Mazor [a] (corresponding author)
matanmazor@outlook.com

Roy Mukamel [a]
rmukamel@post.tau.ac.il

[a] Sagol School of Neuroscience and School of Psychological Sciences, Tel-Aviv University, Tel-Aviv 69978, Israel

Functional magnetic resonance imaging (fMRI) experiments are typically designed to allow the extraction of evoked responses to isolated experimental conditions. At the experimental design level, this is achieved in two ways: randomizing the order of experimental conditions within and between runs, and using a sparse spread of events, allowing for the signal to decay between subsequent events or blocks (with the exception of fast-event related and neural adaptation designs). At the analysis level, a design matrix is constructed with one or more regressors for each experimental condition, and beta weights are then compared in a univariate (single voxel) or multivariate (multi-voxel) manner to assess sensitivity of a particular brain region to the different experimental manipulations. However, often a researcher is less interested in the differences in evoked responses to specific experimental *conditions* (e.g., observation of a red or blue square), but more in the sensitivity of a brain region to the manipulated experimental *dimensions* (e.g., color). To this end, we introduce a novel experimental design and analysis. Together, this new approach allows to infer from asymmetry in the inter-run temporal consistency pattern about sensitivity of single voxels to different experimental dimensions. This approach is model-free, making it appealing for the study of brain regions, populations and experimental manipulations in which assumptions about the hemodynamic response function do not hold. Here we applied it to study the lateralization of hand representation during action-observation. We discuss the possible strengths and limitations of this new approach, in light of our empirical results.

Keywords: fMRI, model-free analysis, multivariate, hand-identity, action observation

1. Introduction

1.1 Model free fMRI analysis

fMRI relies on the coupling between blood flow and neural firing to infer neural activity from blood oxygenation level-dependent (BOLD) signal (Ogawa et al., 1990) - a signal that changes in proportion to the concentration of deoxyhemoglobin in the blood. This signal is correlated with both neural firing and field potentials (Mukamel et al., 2005; Privman et al., 2007), but the mechanisms that underlie this relation are not yet completely understood (Rosa et al., 2015).

The predominant approach to fMRI signal modeling treats the measured fMRI signal as the convolution of neural activity with a Hemodynamic Response Function (HRF), accompanied by Gaussian noise (Boynton et al., 2012). In the past two decades, this linear

transform model has proven very useful. Its simplifying assumptions allow the use of the General Linear Model (GLM), employed in mass univariate Statistical Parametric Mapping (SPM, Friston et al., 1994), and often as a preliminary step to multivariate approaches such as Multi Voxel Pattern Analysis (MVPA, Norman et al., 2006) and Representational Similarity Analysis (RSA, Kriegeskorte et al., 2008).

The assumption of linearity of the BOLD signal is comprised of three assumptions regarding the measured signal (Boynton et al., 2012): being additive (*additivity*), proportional to stimulus salience (*scaling*), and consistent across time-points (*shift invariance*). In addition, it is tacitly assumed that the neurovascular coupling mechanism is consistent across brain regions, thus allowing convolution of the signal from all brain regions with the same canonical HRF.

These assumptions were shown to be reasonable with respect to the human primary visual area (Boynton et al, 1996). However, later work alluded violations of the principles of additivity (Huettel & McCarthy, 2000; Soltysik et al., 2004) and scaling (Vazquez & Noll, 1998). The HRF was also shown to vary between different brain regions (Handwerker et al., 2004, David et al., 2008), and to a lesser degree across time within the same subject (Aguirre et al., 2004). The HRF also varies between populations (D'esposito et al., 2003) such as the elderly (D'esposito et al, 1999; Huettel et al., 2001), children (Richter & Richter, 2003) and clinical patients (Carusone et al, 2002; Fox et al., 2005; H Roder et al., 2010). These facts, which are acknowledged but not commonly taken into account, limit the sensitivity of fMRI model-based analyses, including the widely used GLM. This is especially pertinent when using event-related experimental designs and analysis which are more susceptible to model inaccuracies.

Improving the precision of the model is one solution to this problem. This can be done by allowing more freedom in describing the HRF shape (Rosa et al., 2015) and modeling the deviations from linearity (Monti, 2011). However, one caveat of this approach is that it introduces complications to the model, compromising statistical power and results interpretability (Monti, 2011). An alternative solution is to use model-free approaches, bypassing the need to commit to a specific model. Examples of model-free applications in fMRI analysis include the use of within-subject, inter-voxel correlation as an index of functional connectivity (Biswal et al., 1995, Friston et al., 1996), the use of within-subject, within-voxel correlation for signal reliability assessment across different time points (Hasson et al., 2010), and the use of inter-subject, within-voxel correlations to infer commonalities in a regions' functionality across subjects (Hasson et al., 2004).

All three approaches estimate the correlations between empirical time-series data to learn about brain function. Importantly, these approaches rely on the fact that the time-series are locked to the same series of external events, so that any differences between two time series are inherent to the tissue. In contrast, here we introduce a new approach that examines the asymmetry of temporal consistency in the response pattern across different series of external events (experimental conditions; see table 1). The consistency is examined within subjects, and within voxels. Our method is comprised of two steps. First, the experiment is designed such that experimental runs are consistent with respect to certain experimental dimensions, and are inconsistent with respect to others (TWISTER design; see section 2.1). Second, analysis is performed in a model-free manner, relying on asymmetries in the pattern of temporal consistency between experimental runs as an index of tissue responsiveness to the manipulated dimensions (Temporal Consistency Asymmetry; TCA; see section 2.2).

	Subjects	Voxels	Conditions
Intrasubject reliability (Hasson et al., 2010)	Within	within	within
Intersubject correlation (Hasson et al., 2004)	Between	within	within
Functional connectivity (Biswal et al., 1995)	Within	between	within
TWISTER	**Within**	**within**	**between**

table 1: model-free applications in fMRI analysis

1.2 Body-side mapping in action observation

To test the adequacy of our two-step scheme for neurocognitive research, we applied it to the question of body-side representation in action observation.

A successful extraction of motor information from the observation of others' actions is important for imitation and learning. However, for this extraction to take place, the organism must match between the observed body parts and its own, solving what is known as the *correspondence problem* (Brass & Heiness, 2005). An intriguing question regarding this mapping is whether it adheres to rotational symmetry or to reflection symmetry. Rotational mapping implies that a right-hand movement seen from an allocentric (second person)

viewpoint is mapped to a movement of the observer's right hand (egocentric, first person viewpoint). Conversely, reflection mapping implies that a right-hand movement seen from an allocentric (second person) viewpoint is mapped to a movement of the observer's left hand (as happens when seeing one's own body in the mirror). fMRI studies consistently find reflection-like mapping between egocentric and allocentric perspectives in the anterior superior parietal lobule (SPL): the right SPL responds more strongly for left hand movements when observed from an egocentric perspective, but for right hand movements when observed from an allocentric perspective. An opposite pattern is observed in the left SPL (Shmuelof & Zohary, 2006; Shmuelof & Zohary, 2008; Vingerhoets et al., 2012; Chang et al., 2016). This activation pattern is robust to differences in the visual field in which the hand appears. To the best of our knowledge, no imaging study has successfully identified brain regions that represent body scheme in a manner that adheres to rotational mapping, i.e., that preserves hand identity across perspectives.

Unlike imaging studies, behavioral experiments are more equivocal, providing support for reflection mapping as well as for rotation mapping, depending on context. While mimicry in children younger than 12 years has been shown to adhere to a reflection mapping between self and other, this pattern was attenuated with age (Walpner & Cirillo, 1968). In adults, stimulus-response compatibility effects are better explained by reflection, and not rotational mapping (Vainio & Mustonen, 2011), yet participants were more likely to imitate a model in a rotational manner (even though this made them more prone to errors; Press et al., 2005). Similarly, when facing a walking avatar subjects subconsciously mimicked balance perturbations in a rotational manner (i.e., in response to a right tilt of the avatar, participants tended to tilt to their own right side; Thirioux et al., 2009).

This seeming conflict between imaging and behavioral findings can be due to difference in the nature of the task: the aforementioned behavioral studies included a motor task, as opposed to passive observation inside the MRI scanner. Another possibility is that brain regions that represent body scheme in a manner that complies with rotational mapping could not be detected using available models due to variations in HRF shape or atypical neural dynamics. To investigate this possibility, we designed a TWISTER experiment manipulating rotational (preserving hand identity) and reflection (preserving visual field) mappings as the two dimensions of interest, and used Temporal-Consistency Asymmetry (TCA) to identify asymmetries in the consistency patterns between the resulting time-series. The novel experimental approach and analysis method are detailed below.

2. Materials and Methods

We propose a two-step approach for the study of cognition via fMRI without assuming a specific generative model of the measured signal. Our approach is comprised of an experimental design that manipulates inter-run consistency along specific dimensions of interest (TWISTER, section 2.1), and a quantitative measure of the asymmetry of inter-run consistency in the BOLD response (TCA, section 2.2).

2.1 TWISTER

Unlike traditional experimental designs that are optimized for identifying evoked responses for particular *conditions* or *event-types*, the TWISTER (TWo Independent Stimulus Traits Evenly Randomized) experimental design is optimized for identifying brain regions that are more sensitive to certain *dimensions* along the stimulus space than to other dimensions. A TWISTER experiment is comprised of four experimental runs of equal duration: A1, B1, A2 and B2. The experiment is created in two steps. First, run A1 is formed by randomly dispersing a fixed number of events along a temporal interval of a predefined duration. This step is executed separately for each participant. Second, the three remaining runs are created by taking run A1 as a reference and twisting the events along the first dimension (B1), the second dimension (A2), or both (B2; see fig. 1). The resulting four runs can be used in random order. Thus, when embedded in a space spanned by the two dimensions of interest, run A1 is aligned with run A2 along the first dimension and with run B1 along the second dimension, and the opposite is true for B2.

Consequently, voxels can be embedded in a two dimensional space according to the temporal consistency along the two twisted stimulus dimensions, as reflected in the correlation coefficients between time-series. A brain region whose time-series during run A1 is more consistent (i.e., has higher correlation) with its activation pattern during run A2 than during run B1 is more sensitive to the first dimension (A vs. B) than to the second dimension (1 vs. 2). Similarly, a brain region whose time-series during run B2 is more consistent with its activation pattern during run A2 than during run B1 is more sensitive to the second dimension (1 vs. 2) and less to the first (A vs. B).

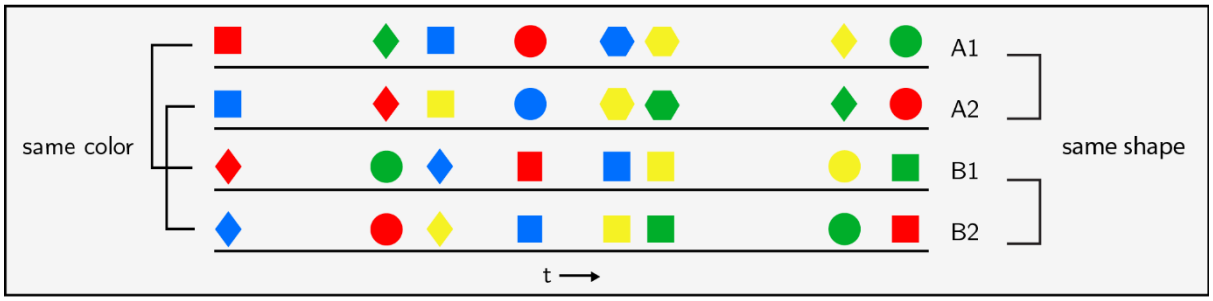

Figure 1. An example of a hypothetical TWISTER experiment, manipulating color and shape as the dimensions of interest. The four lines stand for the four experimental runs. Time progresses along the horizontal axis. Notice that pairs A1, A2 and B1, B2 are consistent with respect to shape but twisted along the color dimension, whereas A1, B1 and A2, B2 are consistent with respect to color but are twisted along the shape dimension. Consequently, a brain region whose activation pattern for A1 is more consistent with its activation pattern for A2 than to B1 can be said to be more sensitive to shape than to color.

2.2 Temporal Consistency Asymmetry (TCA)

TWISTER design allows one to infer from asymmetry in the voxel activation space ('the activation of voxel x during run A1 is more consistent with its activation during run B1 than with its activation during A2') about asymmetry in the voxel's representation space ('voxel x is more sensitive to the second dimension than to the first'). This necessitates a method for comparing temporal consistencies. To quantify the Temporal Consistency asymmetry (TCA) for each voxel, we propose the following procedure:

1. Extract temporal consistency measures.

   For every voxel, do:

   a. Set the *seed time-series* to be the voxel's time-series in a given run (for example, A1). Set the *red-reference* to be the time-series of the same voxel in a different run that is consistent along one dimension but inconsistent along the second dimension (for example, A2). Set the *blue reference* to be the time-series of the same voxel in a different run, consistent only along the second dimension (B1). This step can be done using the concatenation of two standardized time-series, for example setting the concatenation of [A1, B2] as the seed time course, and the concatenation of [A2, B1] and [B1, A2] as red and blue references, respectively.

   b. Compute Pearson's correlation coefficient between each pair of time-series (seed and red reference - r_{SR}; seed and blue reference - r_{SB}; red and blue references - r_{RB}).

c. Set any negative correlation to 0.

2. Extract voxel-wise estimates for the number of independent time points

   To account for temporal autocorrelations in the fMRI time-series, compute the voxel-wise effective sample size (ESS) for each of the three time-series using Neal's approximation (Kass et al., 1998)

$$ESS = N/(1 + 2\sum_{k=1}^{\infty} ACF(k))$$

   Where *N* is the actual number of time-points acquired, and *ACF* is the autocorrelation function for a temporal delay *k*. To obtain a robust estimate for the voxel's ESS, average the three ESS estimates (one for each run), and apply robust spatial smoothing (Garcia, 2010) using ESS estimates of neighboring voxels to reduce random variation.

3. Extract voxel-wise Temporal Consistency Asymmetry (TCA) measures

   For every voxel, do:

   a. Use Hotelling-Williams test (Hotelling, 1940; Williams, 1959) to test the null hypothesis that the seed's temporal consistency with the red reference is equal to its temporal consistency with the blue reference, i.e., $r_{SR} = r_{SB}$, using the formula below:

$$T = (r_{SR} - r_{SB}) \sqrt{\frac{(ESS-1)(1+r_{RB})}{2(\frac{(ESS-1)}{(ESS-3)}|R| + \bar{r}^2(1-r_{BR})^3}}$$

      Where |R| is the determinant of the 3x3 correlation matrix containing the coefficients being tested. This results in a t-value. Positive t-values correspond to $r_{SR} > r_{SB}$ (the seed time-series is more consistent with the red than it is consistent with the blue reference). Similarly, negative values indicate that $r_{SR} < r_{SB}$ (the seed time-series is more consistent with the blue than with the red references).

   b. To generate a voxel-wise p-value, compare the t-statistic against a t-distribution with df = ESS-3

4. Correct for multiple comparisons, and visualize

   a. To address the issue of multiple comparisons, correct p-values for false discovery rate (Benjamini & Yekutieli, 2001).

   b. Color voxels with significantly positive t-values (corresponding to a higher consistency between the seed and the red reference) in red, and voxels with

significantly negative t-values (corresponding to a higher consistency between the seed and the blue reference) in blue.

Step 1.c is included to avoid the interpretation of negative correlations between time-series of the same voxel. While a positive correlation suggests higher consistency than a zero correlation, it is unclear how one should interpret negative correlations in the context of temporal consistency. As an example, consider a voxel whose correlation along the red dimension (r_{SR}) equals -0.6, and its correlation along the blue dimension (r_{SB}) equals 0. Given an effective sample size of 100 and a zero correlation between the red and blue references, the test results with T(97)=-5.0, a significant result in favor of stronger consistency along the blue dimension. This is unwarranted, as the consistency along the blue dimension is null. By setting all negative correlations to 0, we restrict our analysis only to voxels in which the difference between the two correlation coefficients is driven by a positive, and not a negative, correlation.

Our choice to apply voxel-wise, as opposed to cluster-wise correction for multiple comparisons (step 4.a), is driven by our motivation to reduce bias in favor of cortical structures, which are often bigger and spatially smoother compared to subcortical structures.

A Matlab code implementing this analysis scheme is provided, together with the data of one subject, in the supplementary materials for this paper.

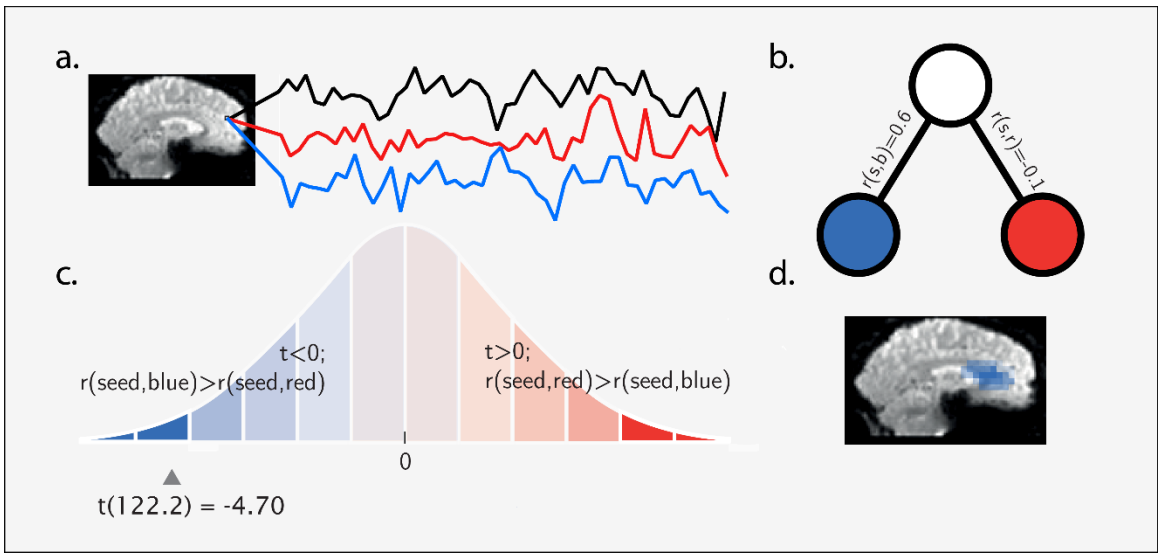

Figure 2. Temporal Consistency Asymmetry (TCA): a. the TCA measure is computed for a given voxel and with respect to three activation time-series (seed = black, red, and blue). b. The analysis is designed to examine whether the seed time-series is more consistent with the red or with the blue

reference time-series. c. Using Hotelling-Williams test and based on the correlation between the three time-series, a t-value is computed. d. The t-value is then compared with the appropriate cumulative distribution function (based on the voxel's ESS, in this case 125.2) to extract a p-value. An SPM is then constructed using voxel-based or cluster-based thresholding, where blue voxels indicate stronger temporal consistency along the blue dimension, and the opposite is true for red voxels.

2.3 Experimental procedure

2.3.1 Participants

Twenty subjects (12 females, ranging from 22 to 33 years old) participated in the experiment. The data of one subject who did not follow the instructions were discarded prior to analysis, and one other subject was recruited to complete an experimental set of 20 subjects. All subjects were right handed (based on self-report), had normal or corrected-to-normal vision, and no reported history of neurological or psychiatric disease. Subjects provided written informed consent to participate in the study and were compensated for their time. The study protocol conformed to the guidelines approved by the Helsinki committee at Sheba Medical Center and the ethics committee of Tel-Aviv University.

2.3.2 fMRI Task

Subjects lay supine on the scanner bed, and viewed visual stimuli back-projected onto a screen through a mirror. Foam pads were used to minimize head motion. Stimulus presentation and timing of all stimuli were achieved using Matlab (Mathworks) and Psychtoolbox (Brainard, 1997; Kleiner et al., 2007; www.psychtoolbox.org). Subjects' eye movements were monitored using an EyeLink 1000 Plus eye-tracker.

The experiment consisted of four 4:34 minutes long experimental runs. During each run, 72 short (1.7 seconds) videos of different hand movements were presented at the center of the screen (see fig. 3a). In each video, one hand rested in a supinated position while the second hand performed one of the following actions: fist opening and closing, fifth digit opposition, fourth digit opposition, third digit opposition or second digit opposition. We used TWISTER design (see section 2.2) to manipulate the inter-run consistency along two dimensions of interest, namely - active hand identity (i.e., action performed by the right hand / left hand) and action visual field (i.e., action appearing on the right visual field / left visual field; manipulated by positioning the camera either in an allocentric position or an egocentric position). Thus, two pairs of runs were aligned along the hand identity dimension, respecting

rotational mapping between egocentric and allocentric perspectives (hereafter, the rotational dimension), and two pairs were aligned along the visual field dimension, respecting reflection mapping between the two perspectives (hereafter, the reflection dimension).

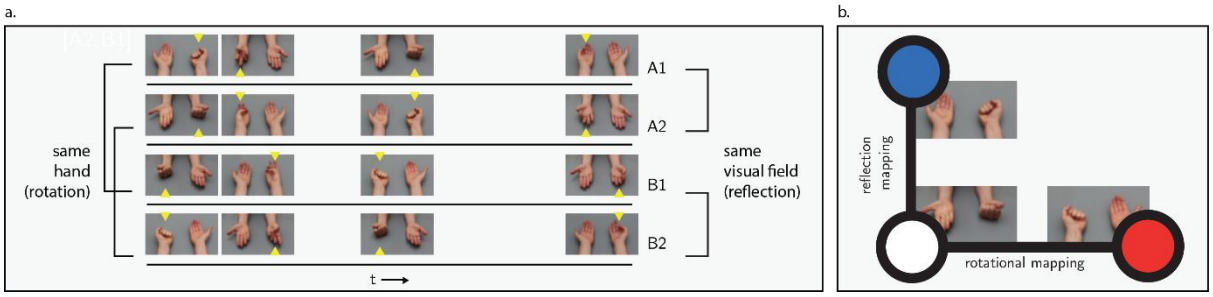

Figure 3. a. Sample screenshots and timeline of the current experiment, manipulating visual field and hand identity as the dimensions of interest. The yellow triangle pointing at the active hand is only presented here for clarity, and was not presented to subjects. In addition, a white fixation cross appeared at the center of the screen throughout the experiment. Importantly, run A1 is identical to run A2 as reflected through a mirror (reflection mapping), and to run B1 as seen from a different perspective (rotation mapping). Likewise, run B2 is identical to run B1 as reflected through a mirror, and to run A2 as seen from a different perspective. b. Three sample stimuli embedded in the space spanned by the reflection and rotational mapping dimensions. With respect to the lower left stimulus, the upper stimulus preserves reflection mapping between egocentric and allocentric perspectives, whereas the right stimulus preserves rotational mapping. Note that for this stimulus set, reflection mapping is equivalent to movement visual field, and rotational mapping is equivalent to active hand identity.

To ensure fixation and to monitor subjects' attention, a white fixation cross appeared in the center of the screen, and participants were asked to covertly count the number of times it rotated throughout the duration of each run. This happened between 3 and 5 times in each run, at random timepoints, not temporally aligned across runs. Subjects reported the number at the end of each run.

2.3.3 MRI Data Acquisition

A Siemens 3-T Prisma scanner (located at the Edersheim-Levi Gitter Center for human brain imaging, Tel Aviv University, Israel) with a 64-channel Siemens Matrix head coil was used to collect all functional and anatomical scans. A single high-resolution structural scan was acquired using a magnetization-prepared rapid acquisition gradient echo (MP-RAGE) sequence (1 x 1 x 1 mm voxels). All functional runs were acquired parallel to the anterior-posterior commissure plane using an echo-planar pulse sequence (38 contiguous interleaved axial slices, 3.5 mm thickness, no gap; TR = 2000 msec; flip angle = 90; TE = 30 msec; in-plane resolution = 3.5 x 3.5 mm; matrix size = 64 x 60).

2.4 Analysis

2.4.1 Image Preprocessing and Statistical Analysis - GLM

The acquired data was analyzed using FEAT v6.00 (FMRI Expert Analysis Tool), part of FSL (FMRIB software library, version 5.0, www.fmrib.ox.ac.uk/fsl). Prior to all preprocessing steps, the first 2 volumes of each run were deleted. Images were then realigned to the central volume of each run to correct for head movements, and spatially smoothed using a 5 mm kernel. The data were then temporally filtered using both a high-pass filter with a cutoff of 50 seconds, and the FILM prewhitening tool. Functional images were registered to the brain-extracted T1 image, using boundary based registration. The anatomical image was registered to the standard MNI space (MNI152, 2mm) by first performing a linear registration with 12 degrees of freedom, and then using the FNIRT nonlinear registration tool with a warp resolution of 10 mm on the linearly registered image.

First level analysis was executed using FILM. The model included 10 regressors: all four conditions, as well as the rare oddball events, were modeled and convolved with a Double-Gamma HRF. These regressors correspond with right hand movement seen from an egocentric perspective (rightEgo), right hand movement seen from an allocentric perspective (rightAllo), left hand movement seen from an egocentric perspective (leftEgo), and left hand movement seen from an allocentric perspective (leftAllo) – collapsed across all five types of hand movements (fist opening and closing, and the four possible digit oppositions). The temporal derivative of each of the resulting regressors was added to the design matrix as a second explanatory variable to account for minor temporal offsets. The design matrix then went through the same temporal filtering process as did the empirical data, before beta values were extracted for each voxel in the brain by fitting the model to the voxels time series. The resulting beta values were then contrasted for each subject using student's t test in a fixed effects model. Single-subject maps were converted to MNI space, and random-effect group level analysis was then performed on the resulting maps, using ordinary least squares (OLS) procedure.

2.4.2 Image preprocessing and statistical analysis - TCA

The preprocessing procedure for the Temporal Consistency Asymmetry analysis differed from the preprocessing for the GLM analysis by only two aspects. In order to

minimize the effects of differences in head orientation due to movement between functional runs, the motion correction procedure used the same reference image for all experimental runs of the same subject, instead of using the central volume of each run as a reference for that particular run. The preprocessing flows also differed in the temporal filtering step: in the absence of a design matrix, the data could not be prewhitened, and so temporal filtering for the TCA analysis consisted only of a highpass filter.

We applied TCA on one triplet of concatenated time-series pairs as described in the results section. In order to account for the different ESS estimates across subjects, t-values were converted to z-values by using the inverse normal cumulative distribution function and multiplying by the sign of the test statistic. Single subject z-maps were converted to MNI space, before group level inference was performed on the normalized z-maps of all 20 subjects using an OLS procedure.

3. Results

3.1 Behavioral task

Performance for the behavioral task was at ceiling.

3.2 GLM

First, we analyzed the results using a conventional GLM method. To examine sensitivity to hand identity irrespective of perspective or visual field, we used the contrast (egoRight+alloRight)-(egoLeft+alloLeft). The contrast highlights brain regions for which the magnitude of activation was explained by a rotation mapping between hands seen from an allocentric and an egocentric perspective. We identified several isolated voxels with a preference for videos in which the right hand was active irrespective of perspective/visual field. These were located at the right superior frontal gyrus, left frontal orbital cortex, left brainstem and left cerebellum. None of these voxels survived FDR correction. No voxel showed a preference for videos in which the left hand was active.

We applied the contrast (egoRight+alloLeft)-(egoLeft+alloRight) to detect regions that are sensitive to the visual field in which the active hand appeared across hand identities and perspectives. The contrast highlights brain regions for which the magnitude of activation was explained by a reflection mapping between hands seen from an allocentric and an egocentric perspective. The right and left lateral occipital and ventral visual cortices showed a

significant preference for hand movements in the left and right visual fields, respectively. In addition, the left superior parietal lobule (SPL) was more activated following hand movements in the right visual field. These clusters survived FDR correction (see Figure 4).

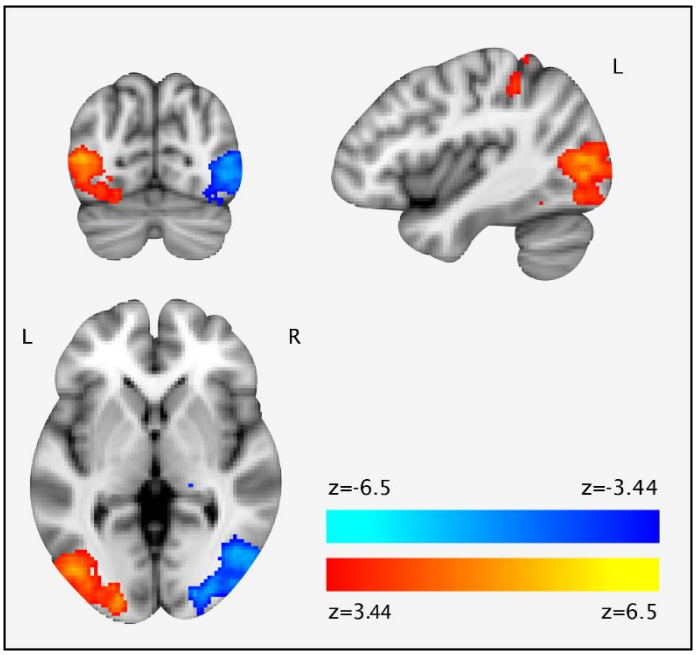

Figure 4. A group level (N=20) GLM contrast of right visual field > left visual field hand movements (reflection mapping), FDR corrected at the single voxel level, q=0.05. L = left, R = right hemisphere

3.3 Whole-brain TCA

We applied TCA to identify regions that are more sensitive to the identity of the perceived active hand (right or left, corresponding to rotational mapping) than to the side on which it appeared on the screen (right or left visual fields, corresponding to reflection-mapping), and vice versa. To this end, we used the time-series concatenation of runs A1 and B2 as our seed time-series, the concatenation of runs B1 and A2 as our red reference, and the concatenation of the same runs in reverse order (A2 and B1) as our blue reference. Thus, with respect to the seed time-series, the red reference was consistent along the rotation (hand-identity) dimension but inconsistent along the reflection (visual-field) dimension, as opposed to the blue reference that was consistent along the reflection (visual-field) dimension, but inconsistent along the rotation (hand-identity) dimension.

This analysis yielded an empty map at the group-level. Thresholding the group-level map at an arbitrary voxel-wise threshold of $p<0.0001$ (two-tailed) revealed two clusters at the bilateral middle temporal (MT) cortex, showing higher consistency along the reflection (blue) than the rotation (red) dimensions (see Table 1). Given their location, these voxels are likely

to respond to the visual field in which the movement appeared. In addition, a relatively small cluster in the right globus pallidus (13 adjacent voxels) showed higher consistency with the red than with the blue references, suggesting a representation of hand identity that adheres to a rotational mapping (i.e., perspective-invariant; see Figures 5 and 6 for single-subject and group results for this comparison, respectively).

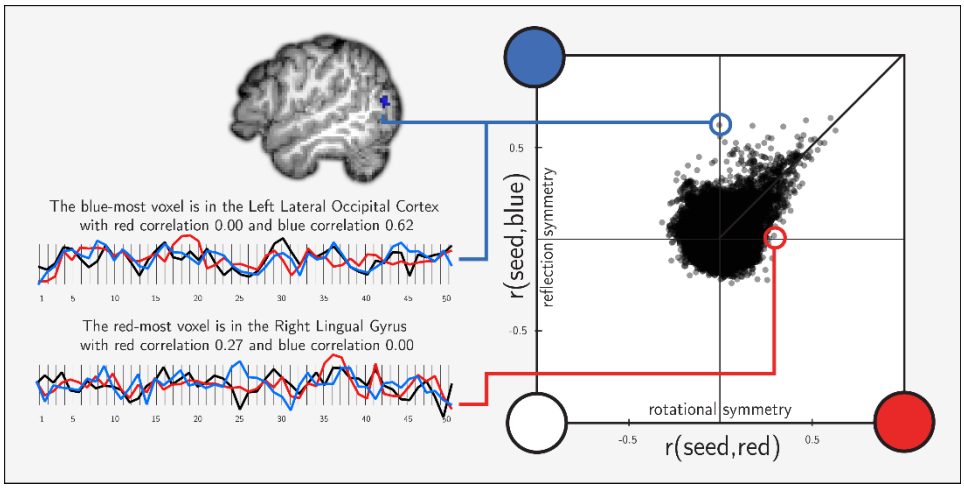

Figure 5. Single subject TCA analysis: Comparing consistency across reflection (blue) and rotation (red) dimensions for one subject. Asymmetry in the temporal consistency is reflected by deviance from the diagonal. Blue voxels survived FDR correction.

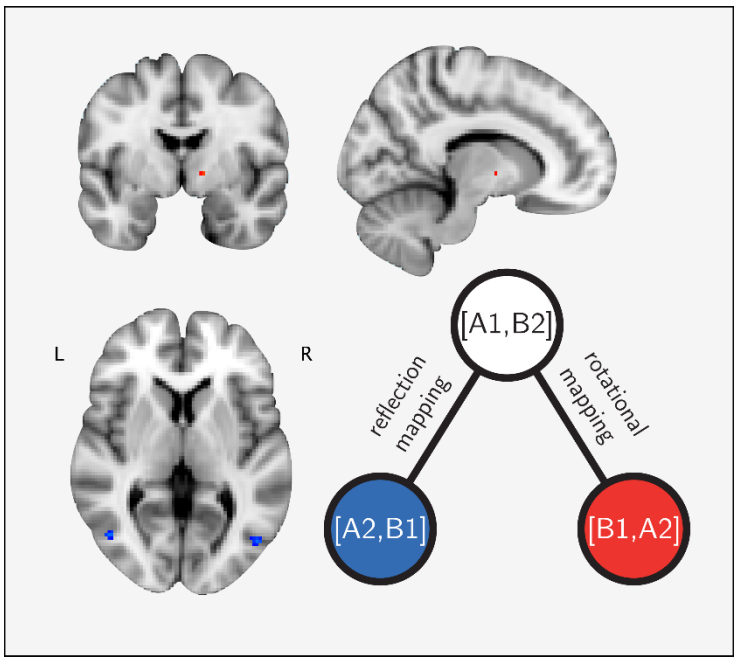

Figure 6. Group level (N=20) TCA analysis. Blue voxels (in area MT) were more consistent along the reflection (visual field) dimension, whereas red voxels (in right globus pallidus) were more consistent

along the rotation (hand-identity) dimension. No voxel survived FDR correction. For visualization purposes only, we used an arbitrary voxel-wise threshold of $p<0.0001$, two-tailed.

Altogether, temporal consistency asymmetries between experimental runs revealed higher consistency along the reflection (visual field) dimension in bilateral MT, and higher consistency along the rotation (hand identity) dimension in the right globus pallidus. However, these results did not survive FDR correction. In an attempt to obtain more conclusive results while controlling for type-I error rates, we ran the same experimental paradigm on an additional set of 10 naïve subjects and used the uncorrected TCA maps from the first 20 subjects as a mask to define regions of interest (ROI) and reduce the number of comparisons.

3.4 ROI-based TCA

3.4.1 Participants

Ten fresh subjects (6 females, ranging from 23 to 28 years old) participated in the second experiment. All subjects were right handed (based on self-report), had normal or corrected-to-normal vision, and no reported history of neurological or psychiatric disease. Subjects provided written informed consent to participate in the study and were compensated for their time. The study protocol conformed to the guidelines approved by the Helsinki committee at Sheba Medical Center and the ethics committee of Tel-Aviv University.

3.4.2 Results

For the second-level analysis we used the uncorrected TCA maps from the first 20 subjects (section 3.2.1) to restrict our analysis to predefined regions of interest. Thus, group-level ROI analysis was performed only on these voxels that exceeded a threshold of $|z|>3.09$, equivalent to $p<0.001$ (one-tailed). Furthermore, group level ordinary least square procedure on the 10 subjects was performed in a one-tailed, instead of two-tailed manner, since we had a specific hypothesis about the direction of the expected effect based on the results from the first 20 subjects.

We observed a significant asymmetry in the temporal consistency pattern of 25 out of 125 voxels and 52 out of 252 voxels in the right and left MT ROIs respectively. These asymmetries were more consistent along the reflection dimension (visual hemifield - blue) than along the rotation dimension (hand identity - red) and survived FDR correction (see Figure 7). Although all 13 voxels in the globus pallidus showed a group level effect in the

expected direction, suggesting compliance with a rotational mapping between perspectives, still no voxel in this ROI survived FDR correction.

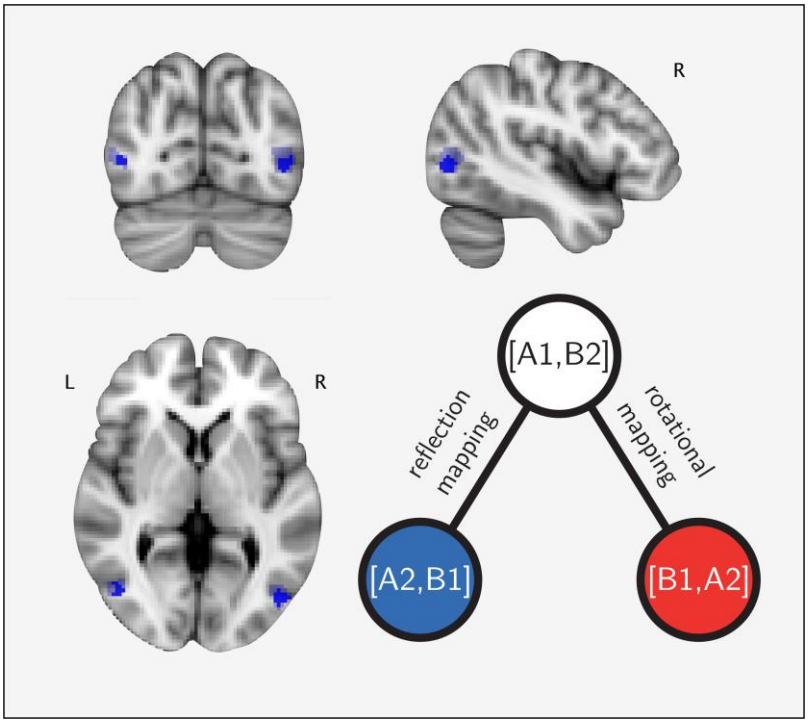

Figure 7. ROI-based group level (N=10) TCA analysis: blue voxels were more consistent along the reflection (visual hemifield) dimension than the rotation (hand identity) dimension. These voxels survived FDR correction after applying the mask obtained from experiment 1.

3.5 Exploratory analysis

3.5.1 Pooled results

We also performed TCA analysis on the joint data from the two subject pools (N=10+20=30). The observed whole-brain map is essentially the same as in the ROI analysis. Bilateral MT responded in a manner that adheres to reflection mapping (FDR corrected), and a trend for rotational mapping is observed in the right globus pallidus ($p<0.00005$, uncorrected).

3.5.2 TCA of model residuals

In order to examine whether our novel method can extract information that is not captured by the standard GLM model, we performed TCA analysis on the residual signal from the GLM analysis. By fitting the design matrix to each voxel's time-series and applying TCA only to the residual time-series, we were able to examine whether the TCA results are driven only by signal dynamics that can be captured by the traditional linear model, or

alternatively, if model-resistant, task related temporal dynamics contribute to the time-series variance in these regions. In the former case, the exclusion of model-compliant dynamics is expected to diminish the TCA results, whereas the latter entails no change in the TCA effect for this intervention.

The bilateral MT clusters did not survive the exclusion of the model-consistent signal, suggesting that most of the temporal dynamics in this region are indeed captured by the linear model. In contrast, the right globus pallidus residual signal behaved in a similar manner to the original signal, still showing a trend for a rotational mapping between perspectives ($p<0.0005$, uncorrected).

4. Discussion

We provide a first proof of concept for a novel approach to fMRI experiment design and analysis. This new scheme is unique in two ways: first, as discussed in the introduction, it is model-free and does not rely on the common assumptions of BOLD linearity or HRF uniformity. Second, TCA provides a statistical framework within the Null Hypothesis Significance Testing for comparing two competing hypotheses specifying different temporal similarity patterns. We first describe our results using this novel approach for a specific experimental question, and then move to discuss general aspects of our method.

We applied this method to the question of interpersonal mapping in action observation. We designed a TWISTER experiment that manipulates both reflection and rotational mappings in an independent manner, and used TCA to detect corresponding asymmetries in the inter-run temporal consistency pattern.

We found a pattern that complies with reflection mapping in the bilateral MT. This pattern is likely to be driven by the presence of motion in the right or left visual hemifields, and is probably not related to any specific representation of body parts or hand movements. In terms of coordinates, the clusters we observed are caudal and medial to the common localization of the adjacent extrastriate body area (EBA; Downing et al., 2004). The temporal consistency asymmetry pattern was primarily governed by dynamics that can be explained by current HRF models, as implied by the fact that this effect diminished when analysis was performed on the model residual time-series, as well as by the fact that the same clusters were revealed using standard mass univariate (GLM) testing.

An opposite pattern was observed in the right globus pallidus, suggesting a rotational mapping between egocentric and allocentric perspectives that is invariant to visual hemifield. This result failed to survive voxel-wise correction for multiple comparisons. In contrast to the cortical clusters, this subcortical pattern was almost unaffected by the removal of the model-consistent signal component. Model-resistant dynamics in the globus-pallidus are compatible with the notion that the typical HRF is less representative of the neurovascular coupling in subcortical regions, but this result should be replicated before any definitive conclusions can be made. A possible explanation for the failure to survive correction for multipole comparisons is the inadequacy of the registration algorithm for the alignment of subcortical structures across subjects. Indeed, here we applied a boundary-based registration algorithm (BBR; Greve & Fischl, 2009) that is optimized for the registration of cortical structures. However, given that voxels in the Globus Pallidus did not survive FDR correction for any of the 30 individual subjects, this explanation can be rejected. Alternatively, the lack of power could be attributed to suboptimal design parameters at the single subject level (such as run length, number of events per run, and the ratio between the two). Further investigation is needed to find the optimal TWISTER design parameters to maximize statistical power.

A GLM contrast of (egoRight+alloLeft)-(egoLeft+alloRight) revealed reflection-like mapping of hands in the left SPL, responding more to movements of the hand corresponding to the participants' right body side. An opposite pattern was observed in the right SPL though this cluster did not survive correction for multiple comparisons. Peak coordinates for these SPL clusters are in line with previous reports of reflection-like representation of moving hands in the anterior SPL (Shmuelof & Zohary, 2006; Shmuelof & Zohary, 2008; Vingerhoets et al., 2012, Chang et al., 2016). Given that previous work demonstrated the robustness of SPL activation to the visual field in which stimuli are presented (Shmuelof & Zohary, 2008), the current SPL activations are unlikely to reflect sensitivity to low-level visual features such as those captured by the MT cortex. The SPL clusters were not identified using TCA. We next turn to discuss different aspects of our novel approach in general.

4.1 TCA vs. other analysis schemes

4.1.1 Advantages of TCA

Serial interactions beyond the single trial

Model-based approaches to fMRI analysis rarely take into account the possible interaction between subsequent events and cognitive processes. Apart from adaptation designs, in which this interaction functions as the dependent measure (e.g., Grill-Spector & Malach, 2001), experimental events are modeled as isolated, independent, and temporally invariant entities. Thus, instead of being explicitly accounted for, interaction between subsequent events is averaged out by trial randomization.

TCA, on the other hand, exploits serial interactions as a source of meaningful information. Temporal multivariate testing, and TCA among them, treats the entire time-series, and not a single event, as one complex datapoint. As the timing and order of events are preserved across runs, any consistent temporal interaction is regarded as a possible source of information instead of noise, be it at the cognitive (Malonie et al., 2005), neural (Wilson et al., 1984) or vascular (Huettel & McCarthy, 2000) levels.

Idiosyncratic patterns

In recent years there has been a movement in the cognitive neuroscience community towards a science that honors differences in responses between different subjects and brain regions (Charest & Kriegeskorte, 2015). The idea of idiosyncratic population codes has led to the wide endorsement of multivariate pattern-information analyses, such as MVPA and RSA. These analyses exploit the high spatial resolution of fMRI, and instead of averaging the signal across voxels they rely on the consistency of spatial activation patterns within categories (MVPA), or across particular tokens (RSA). This way, within-subject spatial consistency can be propagated to population inference even in the presence of idiosyncratic differences in fine-scale anatomy or functional organization (known as "the representational dissimilarity trick"; Kriegeskorte and Kievit, 2013).

While these multivariate analyses allow variation in the spatial organization, they are less tolerant to variations in the *temporal* dynamics of the signal. This is reflected in the extraction of one statistic per voxel. This is done based on some model, either explicitly (as in GLM) or implicitly (as in the choice of the representative time point). In contrast, the proposed analysis scheme uses the consistency of the voxel's time-series across conditions as a measure for its sensitivity to the experimental manipulation. Thus, instead of applying the representational dissimilarity trick spatially, as done in the commonly used MVPA, here we apply it to the temporal dimension. By doing so, TCA is more resilient to model-resistant

activation patterns that may characterize particular brain regions, populations or subjects. This makes TCA less biased for V1-like activation patterns in healthy adults.

Strong null hypothesis

Univariate analysis allows to test both two-tailed ("there is no difference between activation levels in the two conditions") and one-tailed ("activation during condition A is weaker or equal to activation during condition B") hypotheses. Information measures (e.g., classification accuracy) are non-directional, in the sense that they measure how informative/discriminative the activation in a brain region is with regard to the experimental manipulation. They do not allow inference with respect to particular underlying spatio-temporal patterns (Gilron et al., 2017). Thus, information measures such as MVPA only allow to test the null hypothesis that a certain brain region does not hold any information (e.g., cannot discriminate) between the two conditions, equivalent to a univariate two-tailed test. This is a weaker use of the null hypothesis significance testing scheme, as the null hypothesis is less specific, making its rejection more difficult to interpret (Meehl, 1997).

TCA makes a stronger use of hypothesis testing, by putting to test the riskier hypothesis that the sensitivity of a brain region to one dimension is stronger than its sensitivity to another. This is equivalent to a univariate one-tailed test. Putting to test the hypothesis that V4 is more sensitive to shape than to color (a one-tailed hypothesis), is a stronger and riskier use of significance testing than putting to test the hypothesis that v4 is not sensitive to color at all (a two-tailed hypothesis). With high enough statistical power, weak information content (e.g., classification rate of 2% above chance) can come out significant. By comparing sensitivity along two dimensions, information content for the dimension of interest has to exceed that of the baseline dimension for the result to come out significant.

4.1.2. Limitations

Passive experimental procedures

TWISTER design is contingent upon the temporal synchronization between runs. Unlike traditional approaches to fMRI, in which the design matrix can be adapted based on subjects' behavior in the scanner (such as response times, choices or task performance), post-hoc adaptations are not available for TCA analysis, as the design matrix is supplanted by the red and blue reference time-series and the timing of events must be identical across runs. This makes TWISTER less suitable for experimental paradigms in which the timing or type of

events is not experimentally controlled (for example paradigms that rely on subject's responses).

Power

Models increase statistical power by posing a restrictive prior on the space of possible patterns in the signal. While this restriction reduces parameter estimate variance, it also introduces a bias for specific patterns. Model-free approaches are less susceptible to such biases, at the price of a reduction in statistical power. Being model-free, our TCA analysis is more permissive to unexpected temporal patterns in the signal, but is no match for model-based approaches in terms of statistical power.

Thus, when the validity of the model for a set of data is justifiable, one should not be impetuous in turning to model-free approaches, as they are likely to require more subjects or repetitions to detect the same effect. Indeed, in the context of the current study, GLM analysis showed higher sensitivity than the model-free TCA for MT activation. This should be kept in mind, as low powered studies not only compromise the chances of finding an effect when present, but can undermine the reliability of entire lines of research (Button et al., 2013). However, for certain cases, model-free approaches are the only available option for providing insight to what is usually obscured by the model's assumptions. This is the case when dealing with anatomical structures (e.g. subcortical or associative regions), populations (e.g., patients or children), or manipulations (e.g., pharmacological interventions) that are prone to significant deviations from the model.

4.1.3. Other Aspects

You could not step twice into the same river

The brain is a plastic organ, and the first exposure to an event is almost guaranteed to affect the neural responses to future repetitions of the same event (James, 1890, p. 231). Consequently, asymmetries in the temporal consistency between runs may not only reflect true asymmetries in the representational space or random noise, but also systematic differences in processing that stem from run order, such as novelty or habituation effects (generally termed *Groundhog effects*; mcGonigle, 2012). This can be accounted for at the population level (by assigning a different run order to each subject, as done here), and partly at the single-subject level (by splitting each run to two or three sub-runs, and randomizing

their order). However, and not unlike traditional approaches to fMRI analysis, one should always keep in mind possible acquisition order artifacts.

TWISTER design makes it possible to use TCA as a complementary analysis

As demonstrated in the current study (section 2.4), data acquired using a TWISTER design can also be analyzed using mass-univariate GLM testing, in a similar fashion to analysis of data acquired using an event-related experimental design. Importantly, the use of TCA on the GLM residuals can complement the GLM analysis by quantifying the prevalence of evoked responses that could not be captured by the model, thus potentially uncovering regions in which evoked activation patterns do not abide by the assumed model. However, in its original form, TWISTER design violates an important assumption necessary for the application of model-based approaches. Unlike traditional event-related designs, TWISTER does not guarantee that history is balanced across events. However, this can be mitigated by using a standard optimization algorithm to decide on the timing and order of events for run A1, and then twist the events along the different axes to obtain runs A2, B1 and B2.

5. Conclusions

This study provides a first demonstration of a new model-free fMRI application to the study of cognition. We suggest that for some research questions, modeling the predicted evoked responses to single experimental conditions can be superfluous, and statistical inferences can alternatively be made on the time-series as a whole unit, based on its temporal consistency with other time-series. Moreover, circumventing the need for a model makes this approach preferable in cases where model assumptions are violated, as in certain brain regions, populations and interventions.

Our empirical results support the validity of the application of Temporal Consistency Asymmetry (TCA) to TWISTER experimental designs. The results also allude the fact that for model-adequate temporal patterns, model-based approaches are superior in terms of statistical power. Therefore, we suggest that adoption of this method for the study of certain populations (clinical populations, developmental studies), brain regions (subcortical structures, associative cortices) and pharmacological interventions can reduce the literature bias against model-resistant activations.

Acknowledgements: We thank Noam Mazor and Roni Maimon for their useful comments, insights and ideas throughout the development of this new approach. We thank Halely Balaban, Daniel Reznik, Roni Maimon and Batel Buaron, for reading and commenting on the manuscript. Special thanks to the *twitter* and *cross-validated* communities for their invaluable help in different stages of this project.

Aguirre, G. K., Zarahn, E., & D'esposito, M. (1998). The variability of human, BOLD hemodynamic responses. *Neuroimage*, *8*(4), 360-369.

Biswal, B., Yetkin, F. Z., Haughton, V. M., & Hyde, J. S. (1995). Functional connectivity in the motor cortex of resting human brain using echo-planar MRI.*Magnetic resonance in medicine*, *34*(4), 537-541.

Boynton, G. M., Engel, S. A., Glover, G. H., & Heeger, D. J. (1996). Linear systems analysis of functional magnetic resonance imaging in human V1. *The journal of neuroscience*, *16*(13), 4207-4221.

Boynton, G. M., Engel, S. A., & Heeger, D. J. (2012). Linear systems analysis of the fMRI signal. NeuroImage, 62(2), 975-984.

Brass, M., & Heyes, C. (2005). Imitation: is cognitive neuroscience solving the correspondence problem?. *Trends in cognitive sciences*, *9*(10), 489-495

Button, K. S., Ioannidis, J. P., Mokrysz, C., Nosek, B. A., Flint, J., Robinson, E. S., & Munafò, M. R. (2013). Power failure: why small sample size undermines the reliability of neuroscience. *Nature Reviews Neuroscience*,*14*(5), 365-376.

Carusone, L. M., Srinivasan, J., Gitelman, D. R., Mesulam, M. M., & Parrish, T. B. (2002). Hemodynamic response changes in cerebrovascular disease: implications for functional MR imaging. *American Journal of Neuroradiology*,*23*(7), 1222-1228.

Chang, S., Zhang, D., Lin, Y., Xie, S., Li, J., Huang, R. & Liu., M (2016, June). Neural Representations of action observation when changing from egocentric to allocentric viewpoint. Poster session presented at the Annual Convention of the Organization for Human Brain Mapping, Geneva, SUI.

Charest, I., & Kriegeskorte, N. (2015). The brain of the beholder: honouring individual representational idiosyncrasies. *Language, Cognition and Neuroscience*, *30*(4), 367-379.

David, O., Guillemain, I., Saillet, S., Reyt, S., Deransart, C., Segebarth, C., & Depaulis, A. (2008). Identifying neural drivers with functional MRI: an electrophysiological validation.

D'Esposito, M., Zarahn, E., Aguirre, G. K., & Rypma, B. (1999). The effect of normal aging on the coupling of neural activity to the bold hemodynamic response. *Neuroimage*, *10*(1), 6-14.

D'Esposito, M., Deouell, L. Y., & Gazzaley, A. (2003). Alterations in the BOLD fMRI signal with ageing and disease: a challenge for neuroimaging. *Nature Reviews Neuroscience*, *4*(11), 863-872.

Downing, P. E., Jiang, Y., Shuman, M., & Kanwisher, N. (2001). A cortical area selective for visual processing of the human body. *Science*, *293*(5539), 2470-2473.

Fox, M. D., Snyder, A. Z., McAvoy, M. P., Barch, D. M., & Raichle, M. E. (2005). The BOLD onset transient: identification of novel functional differences in schizophrenia. *Neuroimage*, *25*(3), 771-782.

Friston, K. J., Holmes, A. P., Worsley, K. J., Poline, J. P., Frith, C. D., & Frackowiak, R. S. (1994). Statistical parametric maps in functional imaging: a general linear approach. *Human brain mapping*, *2*(4), 189-210.

Friston, K. J., Frith, C. D., Fletcher, P., Liddle, P. F., & Frackowiak, R. S. J. (1996). Functional topography: multidimensional scaling and functional connectivity in the brain. *Cerebral cortex*, *6*(2), 156-164.

Garcia, D. (2010). Robust smoothing of gridded data in one and higher dimensions with missing values. *Computational statistics & data analysis*, *54*(4), 1167-1178

Gilron, R., Rosenblatt, J., Koyejo, O., Poldrack, R. A., & Mukamel, R. (2017). What's in a pattern? Examining the type of signal multivariate analysis uncovers at the group level. *NeuroImage*, *146*, 113-120.

Greve, D. N., & Fischl, B. (2009). Accurate and robust brain image alignment using boundary-based registration. *Neuroimage*, *48*(1), 63-72.

Grill-Spector, K., & Malach, R. (2001). fMR-adaptation: a tool for studying the functional properties of human cortical neurons. *Acta psychologica*, *107*(1), 293-321.

H Roder, C., Marie Hoogendam, J., & M van der Veen, F. (2010). FMRI, antipsychotics and schizophrenia. Influence of different antipsychotics on BOLD-signal. *Current pharmaceutical design*, *16*(18), 2012-2025.

Handwerker, D. A., Ollinger, J. M., & D'Esposito, M. (2004). Variation of BOLD hemodynamic responses across subjects and brain regions and their effects on statistical analyses. *Neuroimage*, *21*(4), 1639-1651.

Hasson, U., Nir, Y., Levy, I., Fuhrmann, G., & Malach, R. (2004). Intersubject synchronization of cortical activity during natural vision. *science*, *303*(5664), 1634-1640.

Hasson, U., Malach, R., & Heeger, D. J. (2010). Reliability of cortical activity during natural stimulation. *Trends in cognitive sciences*, *14*(1), 40-48.

Haxby, J. V., Gobbini, M. I., Furey, M. L., Ishai, A., Schouten, J. L., & Pietrini, P. (2001). Distributed and overlapping representations of faces and objects in ventral temporal cortex. *Science*, *293*(5539), 2425-2430.

Hotelling, H. (1940). The selection of variates for use in prediction with some comments on the general problem of nuisance parameters. *The Annals of Mathematical Statistics*, *11*(3), 271-283.
James, W. (1890)

Huettel, S. A., & McCarthy, G. (2000). Evidence for a refractory period in the hemodynamic response to visual stimuli as measured by MRI. *Neuroimage*,*11*(5), 547-553.

Huettel, S. A., Singerman, J. D., & McCarthy, G. (2001). The effects of aging upon the hemodynamic response measured by functional MRI. *Neuroimage*,*13*(1), 161-175.

Kass, R. E., Carlin, B. P., Gelman, A., & Neal, R. M. (1998). Markov chain Monte Carlo in practice: a roundtable discussion. *The American Statistician*,*52*(2), 93-100.

Kriegeskorte, N., Mur, M., & Bandettini, P. (2008). Representational similarity analysis–connecting the branches of systems neuroscience. *Frontiers in systems neuroscience*, *2*.
Kriegeskorte, N., & Kievit, R. A. (2013). Representational geometry: integrating cognition, computation, and the brain. *Trends in cognitive sciences*, *17*(8), 401-412.

Maloney, L. T., Dal Martello, M. F., Sahm, C., & Spillmann, L. (2005). Past trials influence perception of ambiguous motion quartets through pattern completion. *Proceedings of the National Academy of Sciences of the United States of America*, *102*(8), 3164-3169

McGonigle, D. J. (2012). Test–retest reliability in fMRI: or how I learned to stop worrying and love the variability. *NeuroImage*, *62*(2), 1116-1120.

Meehl, P. E. (1997). The problem is epistemology, not statistics: Replace significance tests by confidence intervals and quantify accuracy of risky numerical predictions.

Monti, M. M. (2011). Statistical analysis of fMRI time-series: a critical review of the GLM approach. *Frontiers in human neuroscience*, *5*(article 28).

Mukamel, R., Gelbard, H., Arieli, A., Hasson, U., Fried, I., & Malach, R. (2005). Coupling between neuronal firing, field potentials, and FMRI in human auditory cortex. Science, 309(5736), 951-954.

Norman, K. A., Polyn, S. M., Detre, G. J., & Haxby, J. V. (2006). Beyond mind-reading: multi-voxel pattern analysis of fMRI data. *Trends in cognitive sciences*, *10*(9), 424-430

Ogawa, S., Lee, T. M., Kay, A. R., & Tank, D. W. (1990). Brain magnetic resonance imaging with contrast dependent on blood oxygenation. Proceedings of the National Academy of Sciences, 87(24), 9868-9872.

Press, C., Ray, E., & Heyes, C. (2009). Imitation of lateralised body movements: doing it the hard way. *Laterality*, *14*(5), 515-527.

Privman, E., Nir, Y., Kramer, U., Kipervasser, S., Andelman, F., Neufeld, M. Y., ... & Malach, R. (2007). Enhanced category tuning revealed by intracranial electroencephalograms in high-order human visual areas. *Journal of Neuroscience*, *27*(23), 6234-6242.

Richter, W., & Richter, M. (2003). The shape of the fMRI BOLD response in children and adults changes systematically with age. *NeuroImage*, *20*(2), 1122-1131.

Rosa, P. N., Figueiredo, P., & Silvestre, C. J. (2015). On the distinguishability of HRF models in fMRI. *Frontiers in Computational Neuroscience*, *9*, 54.

Shmuelof, L., & Zohary, E. (2006). A mirror representation of others' actions in the human anterior parietal cortex. *The Journal of Neuroscience*, *26*(38), 9736-9742.

Shmuelof, L., & Zohary, E. (2008). Mirror-image representation of action in the anterior parietal cortex. *Nature neuroscience*, *11*(11), 1267-1269.

Soltysik, D. A., Peck, K. K., White, K. D., Crosson, B., & Briggs, R. W. (2004). Comparison of hemodynamic response nonlinearity across primary cortical areas. *Neuroimage*, *22*(3), 1117-1127.

Thirioux, B., Jorland, G., Bret, M., Tramus, M. H., & Berthoz, A. (2009). Walking on a line: A motor paradigm using rotation and reflection symmetry to study mental body transformations. *Brain and cognition*, *70*(2), 191-200.

Vazquez, A. L., & Noll, D. C. (1998). Nonlinear aspects of the BOLD response in functional MRI. *Neuroimage*, *7*(2), 108-118.

Vainio, L., & Mustonen, T. (2011). Mapping the identity of a viewed hand in the motor system: Evidence from stimulus–response compatibility. *Journal of Experimental Psychology: Human Perception and Performance*, *37*(1), 207.

Vingerhoets, G., Stevens, L., Meesdom, M., Honoré, P., Vandemaele, P., & Achten, E. (2012). Influence of perspective on the neural correlates of motor resonance during natural action observation. *Neuropsychological rehabilitation*, *22*(5), 752-767.

Wapner, S., & Cirillo, L. (1968). Imitation of a model's hand movements: Age changes in transposition of left-right relations. *Child development*, 887-894.

Williams, E. J. (1959). The comparison of regression variables. *Journal of the Royal Statistical Society. Series B (Methodological)*, 396-399.

Wilson, C. L., Babb, T. L., Halgren, E., Wang, M. L., & Crandall, P. H. (1984). Habituation of human limbic neuronal response to sensory stimulation. *Experimental Neurology*, *84*(1), 74-97

Appendix

Tables 1 and 2: Mask of voxels used for 2nd analysis based on the TCA maps obtained from the first cohort of subjects, thresholded at $p<0.001$. Center of Gravity (COG) coordinates are in MNI space.

TCA red mask:

Cluster Index	Number of Voxels	Max z value in cluster	Max X (vox)	Max Y (vox)	Max Z (vox)	COG X (vox)	COG Y (vox)	COG Z (vox)
1	1	3.18	65	34	10	65	34	10
2	1	3.16	55	50	48	55	50	48
3	2	3.21	52	30	19	52.5	30.5	19
4	6	4.28	63	17	29	62.7	17.5	28.7
5	13	4.17	52	61	36	51.8	61.3	35.7

TCA blue mask:

Cluster Index	Number of Voxels	Max z value in cluster	Max X (vox)	Max Y (vox)	Max Z (vox)	COG X (vox)	COG Y (vox)	COG Z (vox)
1	1	3.11	40	40	8	40	40	8
2	1	3.57	45	43	8	45	43	8
3	1	3.1	45	48	14	45	48	14
4	1	3.1	24	70	20	24	70	20
5	1	3.24	66	60	26	66	60	26
6	1	3.34	34	79	34	34	79	34
7	1	3.25	65	41	37	65	41	37

8	1	3.32	30	80	38	30	80	38
9	1	3.2	65	78	40	65	78	40
10	1	3.25	23	31	45	23	31	45
11	1	3.15	51	87	46	51	87	46
12	1	3.1	78	42	48	78	42	48
13	1	3.37	56	79	48	56	79	48
14	1	3.17	42	92	53	42	92	53
15	1	3.16	35	35	60	35	35	60
16	1	3.16	52	53	60	52	53	60
17	2	3.2	24	68	20	24	68	19.5
18	2	3.13	18	60	24	18	59.5	24
19	2	3.17	29	52	26	28.5	51.5	26
20	2	3.24	25	81	30	25.5	81	30
21	2	3.13	64	81	31	64.5	81	31
22	2	3.33	40	89	31	40	88.5	31
23	2	3.28	28	66	34	27.5	66	34
24	2	3.24	51	37	37	51	37	37.5
25	2	3.21	77	59	39	77	59.5	38.5
26	2	3.34	50	40	42	50.5	39.5	42
27	2	3.5	38	46	48	38	46.5	48
28	2	3.26	78	50	52	78	50	51.5
29	2	3.33	54	70	54	53.5	70	54
30	2	3.15	55	34	55	55	34	55.5
31	2	3.65	55	40	56	55	40	55.5
32	2	3.71	39	67	62	39	67	61.5

33	2	3.23	56	50	63	56	50	63.5
34	3	3.35	48	39	22	48.7	39	21.7
35	3	3.16	58	42	30	57.7	42	29.7
36	3	3.47	13	50	30	13.3	49.7	30
37	3	3.29	40	85	31	40.3	84.7	31
38	3	3.53	42	86	32	42.3	86.6	32
39	3	3.21	42	71	45	42.3	70	44.7
40	3	3.19	49	43	63	48.3	43.3	63
41	3	3.25	42	43	66	42.3	42.7	66
42	4	3.5	20	58	23	20.3	58.5	23.5
43	4	3.3	29	56	27	29.5	56.5	26.5
44	4	3.35	46	91	30	46	90.7	30
45	4	3.79	36	22	50	36.2	22	50
46	4	3.45	49	60	59	49	59	59.7
47	5	3.49	26	57	25	25.4	57	25.8
48	5	3.28	29	49	49	29.2	48.6	48.6
49	7	3.57	38	41	70	37.9	41	69.4
50	7	3.42	54	45	71	53.6	44.6	70.4
51	8	3.52	59	51	31	59.5	50.6	30.6
52	8	4.13	30	42	41	30	42.1	40.7
53	8	3.36	36	28	47	37.2	29.2	46
54	8	3.41	20	25	53	20.6	25.2	53.4
55	8	3.54	40	70	59	39.3	69.8	59.7
56	9	3.36	62	49	26	61.1	48.9	26
57	9	3.58	20	31	43	19.9	31.5	42.7

58	10	3.59	26	56	34	26.3	56.2	34.7
59	10	3.32	43	35	47	42.5	34.5	47.4
60	10	3.63	53	45	61	52.3	44.8	61.3
61	12	3.45	34	19	35	34.8	18.1	34.3
62	12	3.43	64	47	65	62.1	47.2	65.7
63	15	3.54	19	54	29	17.5	53.7	28.7
64	16	3.79	57	19	34	57.1	18.5	33.8
65	19	3.74	51	42	7	50	44	7.46
66	21	3.56	56	54	28	57.2	53.5	28.3
67	22	3.71	44	48	10	44	47.7	10.3
68	125	4.42	68	29	39	68.8	28.4	38.5
69	212	4.36	22	27	38	22.6	26.5	38.6

10. Supplementary Material (code and sample data)

Click here to download 10. Supplementary Material: TWISTER.rar